TECHNICAL REPORT ARLCB-TR-83024

A FUNCTIONAL STRESS INTENSITY
APPROACH TO MULTIPLY CRACKED,
PARTIALLY AUTOFRETTAGED CYLINDERS

S. L. PU

JUNE 1983

US ARMY ARMAMENT RESEARCH AND DEVELOPMENT COMMAND
LARGE CALIBER WEAPON SYSTEMS LABORATORY
BENÉT WEAPONS LABORATORY
WATERVLIET N.Y.   12189

APPROVED FOR PUBLIC RELEASE; DISTRIBUTION UNLIMITED

DTIC QUALITY INSPECTED 5

19970926 013

DISCLAIMER

The findings in this report are not to be construed as an official Department of the Army position unless so designated by other authorized documents.

The use of trade name(s) and/or manufacture(s) does not constitute an official indorsement or approval.

DISPOSITION

Destroy this report when it is no longer needed. Do not return it to the originator.

REPORT DOCUMENTATION PAGE		READ INSTRUCTIONS BEFORE COMPLETING FORM
1. REPORT NUMBER ARLCB-TR-83024	2. GOVT ACCESSION NO.	3. RECIPIENT'S CATALOG NUMBER
4. TITLE (and Subtitle) A FUNCTIONAL STRESS INTENSITY APPROACH TO MULTIPLY CRACKED, PARTIALLY AUTOFRETTAGED CYLINDERS		5. TYPE OF REPORT & PERIOD COVERED Final
		6. PERFORMING ORG. REPORT NUMBER
7. AUTHOR(s) S. L. Pu		8. CONTRACT OR GRANT NUMBER(s)
9. PERFORMING ORGANIZATION NAME AND ADDRESS US Army Armament Research & Development Command Benet Weapons Laboratory, DRDAR-LCB-TL Watervliet, NY 12189		10. PROGRAM ELEMENT, PROJECT, TASK AREA & WORK UNIT NUMBERS AMCMS No. 611102H600011 DA Project No. 1L161102AH60 PRON No. 1A2250041A1A
11. CONTROLLING OFFICE NAME AND ADDRESS US Army Armament Research & Development Command Large Caliber Weapon Systems Laboratory Dover, NJ 07801		12. REPORT DATE June 1983
		13. NUMBER OF PAGES 28
14. MONITORING AGENCY NAME & ADDRESS(If different from Controlling Office)		15. SECURITY CLASS. (of this report) UNCLASSIFIED
		15a. DECLASSIFICATION/DOWNGRADING SCHEDULE

16. DISTRIBUTION STATEMENT (of this Report)

Approved for public release; distribution unlimited.

17. DISTRIBUTION STATEMENT (of the abstract entered in Block 20, If different from Report)

18. SUPPLEMENTARY NOTES

Presented at 28th Conference of Army Mathematicians, Bethesda, Maryland,
28-30 June 1982.
Published in proceedings of the conference.

19. KEY WORDS (Continue on reverse side If necessary and Identify by block number)

Multiple Cracks	Residual Stresses
Thick-Wall Cylinder	Finite Elements
Stress Intensity Factors	Weight Functions

20. ABSTRACT (Continue on reverse side If necessary and identify by block number)

The functional stress intensity approach is presented for a partially auto-frettaged, thick-walled cylinder. This approach is a combination of a series of methods developed for the computation of stress intensity factors for multiple-radial cracks emanating from the inner or the outer surface of a hollow cylinder. The numerical method is mainly based on the finite element method using 12-node quadrilateral, isoparametric elements with singular

(CONT'D ON REVERSE)

DD _{1 JAN 73} FORM 1473   EDITION OF 1 NOV 65 IS OBSOLETE

20. ABSTRACT (Cont'd)

elements around a crack tip. The difficulty due to the presence of initial stresses in the finite element method is obviated by the method of thermal simulation which replaces the residual stresses existing in an autofrettaged cylinder by an active thermal load. The weight function method is incorporated to reduce the repeated computations of stress intensity factors of the same geometrical configuration subjected to various external loads and residual stresses. The functional stress intensity factor is introduced to overcome the difficulty in seeking the weight function itself.

Numerical results of functional stress intensity factors are given for multiple cracks radiating from the bore or from the outer surface of a cylinder having an external diameter twice that of an internal diameter. A linear superposition of these results gives the resultant stress intensity factor of a cracked geometry subjected to combined external loads and initial stresses. It is highly possible to extend the method outlined in this report for elastic-perfectly plastic material to strain-hardening materials.

TABLE OF CONTENTS

LIST OF ILLUSTRATIONS

INTRODUCTION

An analytic method is not available for the computation of stress intensity factors for multiple-radial cracks in a thick-walled cylinder. The computation must depend on various numerical methods.[1-5] Due to increasingly successful applications of the finite element technique in structural analysis, the author decided to use higher order finite elements with the aid of special crack-tip elements to study multiply cracked cylinders. Similar to the quarter-point element in an 8-node quadrilateral element,[6,7] a special crack-tip element was developed[8] for a 12-node quadrilateral, isoparametric element. Both the 8-node and 12-node quadrilaterals have been implemented in the popular finite element computer code NASTRAN.[8,9] The dummy user element facility of NASTRAN is used for the implementation. Another finite element computer code APES,[10] which was written specifically for the use of 12-node quadrilateral, isoparametric elements, has also been used for fracture analysis of cracked hollow cylinders. Quite accurate results of stress intensity factors have been obtained using either NASTRAN or APES for multiple-radial cracks emanating from the bore of a tube.[11] These results are in good agreement with results reported by Tracy[12] using the method of modified mapping collocation.

To increase the maximum internal pressure a cylinder can contain elastically and retard the growth of radial cracks near the bore, it is a common practice to introduce compressive residual stress near the bore by an autofrettage process. However, the residual stress in the cylinder causes

References are listed at the end of this report.

1

increased difficulties in the estimation of stress intensity factors. One of the difficulties is that results of residual stress distribution vary based on different assumptions by different investigators. Another difficulty is the lack of an initial stress analysis capability in NASTRAN and APES. A method is developed in Reference 13 so that NASTRAN or APES can be used for the computation of stress intensity factors for cracked cylinders with residual stress distribution given in the closed form expressions.[14] The finite element results[15] are in close agreement with Parker's results[16] using modified mapping collocation.

While the autofrettage process produces favorable compressive residual stress near the bore, it also yields a tensile residual stress near the outer cylindrical surface. The sum of this stress and the tensile stress due to a bore pressure may be high enough to cause crack initiation and propagation from the outer surface of the cylinder. This requires the computation of stress intensity factors for externally cracked cylinders. Several investigators have reported their results on this subject.[12,17-19]

In order to reduce repeated finite element computations, the weight function method[20] is used together with the finite element method. In this report the functional stress intensity factor approach is summarized for both internally cracked and externally cracked, partially autofrettaged, pressurized thick-walled cylinders.

2

RESIDUAL STRESSES AND THERMAL SIMULATION

The residual stress distribution in an autofrettaged thick-walled cylinder has been studied by a large number of investigators. There is considerable disagreement in their results due to different assumptions which must be made in order to make the problem mathematically tractable. Detailed discussions of the results and the associated assumptions are given in References 14 and 21. Under the combination of assumptions that the material is incompressible, elastic-perfectly plastic, and obeys the von Mises' yield criterion, and that the cylinder is under the condition of plane strain, the following closed form solution for residual stresses is obtained for an elastically unloaded cylinder after partial autofrettage:

$$
\sigma_r(r) = \begin{cases} \dfrac{\sigma_o}{\sqrt{3}}\{2 \log \dfrac{r}{\rho} - 1 + \dfrac{\rho^2}{b^2} - P_1(\dfrac{1}{b^2} - \dfrac{1}{r^2})\} & 1 < r < \rho \qquad (1) \\[4mm] \dfrac{\sigma_o}{\sqrt{3}} (\rho^2 - P_1)(\dfrac{1}{b^2} - \dfrac{1}{r^2}) & \rho < r < b \qquad (2) \end{cases}
$$

$$
\sigma_\theta(r) = \begin{cases} \dfrac{\sigma_o}{\sqrt{3}}\{2 \log \dfrac{r}{\rho} + 1 + \dfrac{\rho^2}{b^2} - P_1(\dfrac{1}{b^2} + \dfrac{1}{r^2})\} & 1 < r < \rho \qquad (3) \\[4mm] \dfrac{\sigma_o}{\sqrt{3}} (\rho^2 - P_1)(\dfrac{1}{b^2} + \dfrac{1}{r^2}) & \rho < r < b \qquad (4) \end{cases}
$$

where bore radius is taken as unit length, b is the outer radius of the hollow cylinder, ρ is the radius of the elastic-plastic interface during pressurization, σ_o is the uniaxial yield stress in tension and compression, and

$$
P_1 = P_1(\rho) = \frac{b^2}{b^2-1} (1 - \frac{\rho^2}{b^2} + 2 \log \rho) \qquad (5)
$$

3

This residual stress distribution is used in this report as a basis to develop a method to compute stress intensity factors for cracks in such a stress field. It has been shown in Reference 13 that the thermal stresses in the cylinder subjected to a thermal load

$$
T(r) = \begin{cases} T_O - \dfrac{(T_O - T_\rho)}{\log \rho} \log r & 1 \leqslant r \leqslant \rho \\[4mm] T_\rho & \rho \leqslant r \leqslant b \end{cases} \tag{6}
$$

are equivalent to the residual stresses in Eqs. (1) through (4) if the temperature gradient and the yield stress satisfy

$$
\frac{E\alpha(T_O - T_\rho)}{2(1-\nu)\log \rho} = \frac{2\sigma_O}{\sqrt{3}} \tag{7}
$$

where T_O and T_ρ are the temperatures at the bore, and $r = \rho$ respectively, E is Young's modulus, and α is the coefficient of linear thermal expansion. This thermal simulation provides an effective method to compute stress intensity factors due to initial stresses given by Eqs. (1) through (4) using NASTRAN or APES. The initial stress is replaced by a temperature input of Eq. (6) at all nodes. The stress intensity factors obtained from NASTRAN or APES corresponding to the thermal loads are equivalent to stress intensity factors due to autofrettage residual stresses.[22]

WEIGHT FUNCTION AND FUNCTIONAL STRESS INTENSITY

A weight function is a universal function which depends only on geometry and not on loadings.[20] If the mode I stress intensity factor $K^{(1)}$ and displacement field $\underline{u}^{(1)}$ associated with the symmetric load system 1 are known, the weight function for the cracked geometry is

4

$$h = \frac{H}{2K^{(1)}(c)} \frac{\partial u^{(1)}(c)}{\partial c} \tag{8}$$

where $H = E$ for plane stress and $H = E/(1-\nu^2)$ for plane strain; c is the crack depth. Once h is determined, the mode I stress intensity factor induced by any other symmetric load system τ and f is given by

$$K = \int_\Gamma (\tau \cdot h) d\Gamma + \int_A (f \cdot h) dA \tag{8a}$$

where τ is the stress vector acting on boundary Γ around the crack tip and f is the body force in region A defined by Γ. This equation can be reduced to

$$K = \frac{H}{K^{(1)}} \int_0^c p_c(x) \frac{\partial v^{(1)}}{\partial c} dx \tag{9}$$

for radially cracked rings with x being a distance measured along the crack from the base toward the tip. The relation between r and x is

$$r(x) = \begin{cases} 1 + x & , \text{ for interior cracks} \\ b - x & , \text{ for exterior cracks} \end{cases} \tag{10}$$

The crack pressure $p_c(x)$ can be found from the hoop stress (at the site of radial cracks) in an uncracked ring subjected to the loading of interest. Even though the numerical values of $K^{(1)}$ and $v^{(1)}$, the normal component of displacement, are known, the partial derivative $\partial v^{(1)}/\partial c$ is usually unknown. A technique of computing $\partial v/\partial c$ was devised in Reference 3 by assuming the crack face displacement v be a conic section given by Orange.[23] Another method developed in Reference 15 made no assumptions on v or $\partial v/\partial c$, but utilized the finite element method to compute several stress intensity factors each associated with a simple loading system. For a new load, the new K is expressed in terms of known values of K.

The hoop stress in an uncracked cylinder subjected to an internal pressure p_i is

$$\frac{\sigma_\theta(r)}{p_i} = \frac{1}{b^2-1} \left(1 + \frac{b^2}{r^2}\right) \tag{11}$$

Substituting σ_θ from Eq. (11) as p_c in Eq. (9) we have

$$\frac{K(p_i)}{p_i} = \frac{1}{b^2-1} K_c(1) + \frac{b^2}{b^2-1} K_c(r^{-2}) \tag{12}$$

where

$$K_c(1) = \frac{H}{K(1)} \int_o^c \frac{\partial v(1)}{\partial c} dx \tag{13}$$

$$K_c(r^{-2}) = \frac{H}{K(1)} \int_o^c [r(x)]^{-2} \frac{\partial v(1)}{\partial c} dx \tag{14}$$

are called functional stress intensity factors.

Similarly we get

$$\frac{K(p_o)}{p_o} = \frac{b^2}{b^2-1} K_c(1) + \frac{b^2}{b^2-1} K_c(r^{-2}) \tag{15}$$

$$\frac{K(\rho=b)}{\sigma_o} = \frac{1}{\sqrt{3}} \{[2 - P_1(b)]K_c(1) - P_1(b)K_c(r^{-2}) + 2K_c(\log r)\} \tag{16}$$

for the same cylinder subjected to uniform tension p_o on outer cylindrical surface and fully autofrettaged residual stress respectively. In Eq. (16) the new functional stress intensity factor is

$$K_c(\log r) = \frac{H}{K(1)} \int_o^c \log(r(x)) \frac{\partial v(1)}{\partial x} dx \tag{17}$$

6

The finite element results of $K(p_1)/p_1$, $K(p_0)/p_0$ and $K(\rho=b)/\sigma_0$ enable us to compute the functional stress intensity factors $K_c(1)$, $K_c(r^{-2})$, and $K_c(\log r)$. For the same flawed cylinder with a different degree of autofrettage, the stressses can be computed from one of the following algebraic equations. For an inner crack with the crack tip r_c in the range $1 \leqslant r_c \leqslant \rho$, the equation is

$$\frac{K(\rho)}{\sigma_0} = \frac{1}{\sqrt{3}} \{[2 - P_1(\rho)]K_c(1) - P_1(\rho)K_c(r^{-2}) + 2K_c(\log r)\} \qquad (18)$$

For an outer crack with r_c in the range $\rho \leqslant r_c \leqslant b$, the equation is

$$\frac{K(\rho)}{\sigma_0} = \frac{1}{\sqrt{3}} [\rho^2 - P_1(\rho)][b^{-2}K_c(1) + K_c(r^{-2})] \qquad (19)$$

MODIFICATION FORMULAS

For a partially autofrettaged cylinder, let ε be the degree of auto-frettage, then $\varepsilon = (\rho-1)/t$ where $t = b - 1$ is the wall thickness of the cylinder. When a crack crosses the elastic-plastic interface $r = \rho$, the hoop stress along the crack face must be represented by both Eqs. (3) and (4). Hence Eqs. (18) and (19) are not valid in such a situation. For inner cracks, we may use Eq. (18) to compute an approximate value which is based on the crack face loading of Eq. (3). The error introduced by Eq. (18) may be corrected by adding the following crack face loading

$$p_c(r) = \begin{cases} 0, & 1 \leqslant r \leqslant \rho \\ \frac{\sigma_0}{\sqrt{3}} (\rho^2 - P_1)(\frac{1}{b^2} + \frac{1}{r^2}) - \frac{\sigma_0}{\sqrt{3}} \{2 \log \frac{r}{\rho} + 1 + \frac{\rho^2}{b^2} - P_1(\frac{1}{b^2} + \frac{1}{r^2})\}, & \rho \leqslant r \leqslant r_c \end{cases}$$

$$(20)$$

where r_c is the radius of the crack tip. Substituting from the above into Eq. (9), we should be able to obtain a correction stress intensity factor K_δ if $\partial v/\partial c$ is known. Assume the crack tip crosses the elastic-plastic interface only slightly, the Westergaard near field solution for v in terms of crack-tip stress intensity factor $K^{(1)}$ can be approximately used to find $\partial v/\partial c$. Let ξ be a length measured from the crack tip and be defined by

$$\xi = -(x-c) \tag{21}$$

then

$$v(\xi) = \frac{2K^{(1)}}{H} \left(\frac{2}{\pi}\right)^{1/2} \sqrt{\xi} \tag{22}$$

and

$$\frac{\partial v}{\partial c} = \frac{K^{(1)}}{H} \left(\frac{2}{\pi}\right)^{1/2} \left(-\frac{1}{\sqrt{\xi}} + \frac{1}{c} \sqrt{\xi}\right) \tag{23}$$

The approximate correction factor K_δ obtained by termwise integration of Eq. (9) using Eqs. (20) and (23) is given by

$$\frac{K_\delta}{\sigma_o} = \frac{1}{\sqrt{3}} \sqrt{2/\pi} \{-1 + 2 \log \rho)(I_1 + I_1') + \rho^2(I_2 + I_2') - 2(I_3 + I_3')\} \tag{24}$$

Using $\delta t = |r_c - \rho|$, the abbreviations in Eq. (24) are:

$$I_1 = 2\sqrt{\delta t} \quad , \quad I_1' = \frac{2}{3c} (\delta t)^{3/2} \tag{25}$$

$$I_2 = \frac{1}{1+c} \left[\frac{\sqrt{\delta t}}{\rho} - \frac{(1+c)^{-1/2}}{2} \log D(\rho)\right]$$

$$\tag{26}$$

$$I_2' = \frac{1}{c} \left[\frac{\sqrt{\delta t}}{\rho} + \frac{(1+c)^{-1/2}}{2} \log D(\rho)\right]$$

8

$$I_3 = -2[(2-\log \rho)\sqrt{\delta t} + (1+c)^{1/2} \log \frac{\sqrt{1+c} - \sqrt{\delta t}}{\sqrt{1+c} + \sqrt{\delta t}}]$$

(27)

$$I_3' = \frac{2}{3c} [\sqrt{\delta t} \{\delta t \log \rho - 2(1+c) - 2\delta t/3\} - (1+c)^{3/2} \log D(\rho)]$$

with

$$D(\rho) = [2(1+c) - \rho - 2\sqrt{\delta t(1+c)}]/\rho \qquad (28)$$

The sum of K_δ/σ_0 from Eq. (24) and $K(\rho)/\sigma_0$ from Eq. (18) usually gives a better approximation of crack-tip stress intensity factors when $\delta = |r_c - \rho|/t$ is small. Since the correction formula K_δ/σ_0 is not a function of N, the number of cracks, it works for small N and δ. But when N is large, the crack interaction is strong, and δ must be small.

A similar formula can be found for exterior cracks crossing the elastic-plastic interface from elastic into plastic region.

$$\frac{K_\delta}{\sigma_0} = (\frac{2}{3\pi})^{1/2}\{(1-2 \log \rho)(J_1+J_1') - \rho^2(J_2+J_2') + 2(J_3+J_3')\} \qquad (29)$$

where

$$J_1 = 2\sqrt{\delta t} \quad , \quad J_1' = \frac{2}{3c} (\delta t)^{3/2} \qquad (30)$$

$$J_2 = \frac{1}{r_c} [\frac{\sqrt{\delta t}}{\rho} + r_c^{-1/2} \tan^{-1}\sqrt{\delta t/r_c}] \qquad (31)$$

$$J_2' = \frac{1}{c} [- \frac{\sqrt{\delta t}}{\rho} + r_c^{-1/2} \tan^{-1}\sqrt{\delta t/r_c}] \qquad (32)$$

$$J_3 = 2[(-2+\log \rho)\sqrt{\delta t} + 2\sqrt{r_c} \tan^{-1}\sqrt{\delta t/r_c}] \qquad (33)$$

$$J_3' = \frac{2}{3c} [(\delta t)^{3/2}\log \rho + \frac{2}{3} (3r_c-\delta t)\sqrt{\delta t} - 2r_c^{3/2} \tan^{-1}\sqrt{\delta t/r_c}] \qquad (34)$$

9

Adding K_δ/σ_0 of Eq. (29) to $K(\rho)/\sigma_0$ of Eq. (19), the result is the corrected crack-tip stress intensity factors for exterior cracks.

NUMERICAL RESULTS AND CONCLUSIONS

Extensive numerical results are obtained for a cylinder of $b = 2$, which is a commonly used value in cannon design. A typical finite element idealization is shown in Figure 1 for inner radial cracks. Slight modifications in element meshes are needed for exterior cracks. In Figure 1 the elements surrounding the crack tip are enriched elements.[10] If collapsed singular elements are to be used, we can simply replace the enriched quadrilaterals by collapsed quadrilateral elements (triangular elements) with proper shifting of side nodes to new locations. Similar accuracy is achieved using either enriched or collapsed quadrilaterals. Stress intensity factors for internal cracks are given in Table 1 of Reference 15 for three different types of loadings. Using these results and using Eqs. (12), (15), and (16), we obtain functional stress intensity factors for internal cracks. Figure 2 shows stress intensity factors as a function of c/t for various numbers of internal cracks in a fully autofrettaged cylinder. Figures 3, 4, and 5 are similar graphs of functional stress intensity factors. Corresponding graphs for external cracks are shown in Figures 6 through 9.

Readings taken from Figures 3, 4, and 5 are enough for an estimate of stress intensity factor for internally cracked cylinders with any assigned values of N and c/t for any combination of p_i and residual stresses corresponding to a given ε. If crack tips cross the elastic-plastic

10

interface, then correction formula (24) should be used. As an example, if the stress intensity factor is desired for $N = 2$, $c/t = 0.3$ in a 25 percent autofrettaged cylinder, we first take readings: $K_c(1)/\sqrt{\pi c} = 1.41$ from Figure 3, $K_c(r^{-2})/\sqrt{\pi c} = 1.05$ from Figure 4, and $K_c(\log r)/\sqrt{\pi c} = 0.22$ from Figure 5; then $K_c(\varepsilon=0.25)/\sigma_0\sqrt{\pi c} = -0.12$ is computed from Eq. (18). Since $r_c = 1.3$ is greater than $\rho = 1.25$, the correction stress intensity factor $K_\delta/\sigma_0\sqrt{\pi c} = -0.023$ is obtained from Eq. (24). The sum of Eqs. (18) and (24) gives $K/\sigma_0\sqrt{\pi c} = -0.143$. To check this result, a finite element computation of this case is performed. The result is also -0.143. For externally cracked cylinders, Eq. (19) involves only two functional stress intensity factors. Therefore, only Figures 7 and 8 are needed. For example, given $N = 4$, readings taken from Figure 7 are $K_c(1)/\sqrt{\pi c} = 1.12$ and 1.18 for $c/t = 0.2$ and 0.3 respectively. Readings are $K_c(r^{-2})/\sqrt{\pi c} = 0.32$ for $c/t = 0.2$ and 0.36 for $c/t = 0.3$ from Figure 8. Stress intensity factors for $\varepsilon = 0.8$ can be computed from Eq. (19), giving $K(\varepsilon=0.8)/\sigma_0\sqrt{\pi c} = 0.492$ and 0.537 for $c/t = 0.2$ and 0.3 respectively. For $c/t = 0.3$, the correction formula (29) must be used. The result is $K_\delta/\sigma_0\sqrt{\pi c} = -0.05$. The final result for $c/t = 0.3$ is $K(\varepsilon=0.8)/\sigma_0 = 0.487$ which is close to the result of 0.486 obtained directly from a finite element computation.

For a combination of residual stresses and internal pressure, the stress intensity factor is simply an algebraic sum. Stress intensity factors normalized by $\sigma_0\sqrt{\pi c}$ are shown in Figure 10 as a function of N for internal cracks subjected to several selected values of p_i and ε. Figure 11 is a similar graph for external cracks.

The functional stress intensity factors are used to obviate the difficulty in finding the weight function itself. The approach is the result of a series of methods developed for multiply cracked cylinders. The extension of the method to residual stress distribution other than that given by Eqs. (1) through (4) is highly possible.

From numerical results, the stress intensity factor is largest for $N = 2$ for various combinations of residual stresses and internal pressures for both interior and exterior cracks. The stress intensity factor monotonically decreases as the number of cracks increases from $N = 2$.

REFERENCES

1. Bowie, O. L. and Freese, C. E., "Elastic Analysis For a Radial Crack in a Circular Ring," Engineering Fracture Mechanics, Vol. 4, 1972, pp. 315-321.

2. Shannon, R. W. E., "Stress Intensity Factors For Thick-Walled Cylinders," International Journal of Pressure Vessels and Piping, Vol. 2, 1974, pp. 19-29.

3. Grandt, A. F., "Two Dimensional Stress Intensity Factor Solutions For Radially Cracked Rings," Technical Report AFML-TR-75-121, Air Force Materials Laboratory, 1975.

4. Goldthorpe, B. D., "Fatigue and Fracture of Thick-Walled Cylinders and Gun Barrels," Case Studies in Fracture Mechanics, Technical Report AMMRC-MS 77-5, Army Mechanics and Materials Research Center, 1977.

5. Baratta, F. I., "Stress Intensity Factors for Internal Multiple Cracks in Thick-Walled Cylinders Stressed by Internal Pressure Using Load Relief Factors," Engineering Fracture Mechanics, Vol. 10, 1978, pp. 691-697.

6. Henshell, R. D. and Shaw, K. G., "Crack Tip Finite Elements are Unnecessary," Int. J. for Numerical Methods in Engineering, Vol. 9, 1975, pp. 495-507.

7. Barsoum, R. S., "On the Use of Isoparametric Finite Elements in Linear Fracture Mechanics," Int. J. for Numerical Methods in Engineering, Vol. 10, 1976, pp. 25-37.

8. Pu, S. L., Hussain, M. A., and Lorensen, W. E., "The Collapsed Cubic Isoparametric Element as a Singular Element for Crack Problems," Int. J. for Numerical Methods in Engineering, Vol. 12, 1978, pp. 1727-1742.

9. Hussain, M. A., Lorensen, W. E., and Pflegl, G., "The Quarter-Point Quadratic Isoparametric Element as a Singular Element For Crack Problems," NASA TM-X-3428, 1976, p. 419.

10. Gifford, L. N. Jr., "APES - Second Generation Two-Dimensional Fracture Mechanics and Stress Analysis By Finite Elements," Report 4799, David Taylor Naval Ship Research and Development Center, 1975.

11. Pu, S. L. and Hussain, M. A., "Stress Intensity Factors For a Circular Ring With Uniform Array of Radial Cracks Using Cubic Isoparametric Singular Elements," Fracture Mechanics, ASTM STP 677, 1979, pp. 685-699.

12. Tracy, P. G., "Elastic Analysis of Radial Cracks Emanating From the Outer and Inner Surfaces of a Circular Ring," Engineering Fracture Mechanics, Vol. 11, 1979, pp. 291-300.

13. Hussain, M. A., Pu, S. L., Vasilakis, J. D., and O'Hara, P., "Simulation of Partial Autofrettage By Thermal Loads," Journal of Pressure Vessel Technology, Vol. 102, No. 3, 1980, pp. 314-318.

14. Hill, R., The Mathematical Theory of Plasticity, Oxford at the Clarendon Press, 1950.

15. Pu, S. L. and Hussain, M. A., "Stress Intensity Factors For Radial Cracks in a Partially Autofrettaged Thick-Wall Cylinder," Proceedings of 14th National Symposium on Fracture Mechanics, 1981.

16. Parker, A. P. and Andrasic, C. P., "Stress Intensity Prediction For a Multiply-Cracked, Pressurized Gun Tube With Residual and Thermal Stresses," Army Symposium on Solid Mechanics, AMMRC MS 80-5, 1980, pp. 35-39.

17. Kapp, J. A. and Eisenstadt, R., "Crack Growth in Externally Flawed, Autofrettaged Thick-Walled Cylinders and Rings," Fracture Mechanics, ASTM STP 677, 1979, pp. 746-756.

18. Parker, A. P., "Stress Intensity and Fatigue Crack Growth in Multiply-Cracked, Pressurized, Partially Autofrettaged Thick Cylinders," AMMRC TR 81-37, 1981.

19. Pu, S. L., "Stress Intensity Factors For Radial Cracks at Outer Surface of a Partially Autofrettaged Cylinder Subjected to Internal Pressure," USA ARRADCOM Technical Report ARLCB-TR-82003, Benet Weapons Laboratory, Watervliet, NY, 1982.

20. Rice, J. R., "Some Remarks on Elastic Crack-Tip Stress Fields," Int. Journal of Solids and Structures, Vol. 8, 1972, pp. 751-758.

21. Davidson, T. E. and Kendall, D. P., "The Design of Pressure Vessels For Very High Pressure Operation," Mechanical Behavior of Materials Under Pressure, Edited by H. L. D. Pugh, Elsevier Co., 1970.

22. Pu, S. L. and Hussain, M. A., "Residual Stress Redistribution Caused by Notches and Cracks in a Partially Autofrettaged Tube," Journal of Pressure Vessel Technology, Vol. 103, No. 4, 1981, pp. 302-306.

23. Orange, T. W., "Crack Shapes and Stress Intensity Factors For Edge-Cracked Specimens," ASTM STP 513, 1972, pp. 71-78.
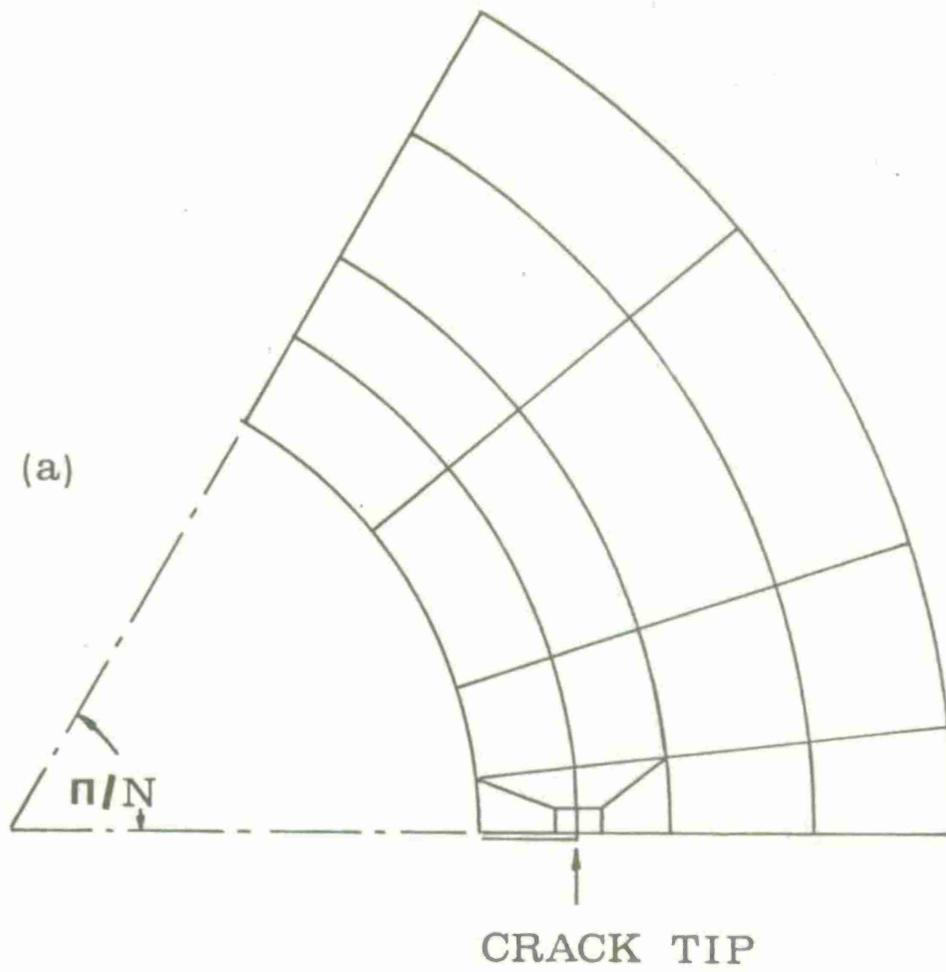
CRACK TIP

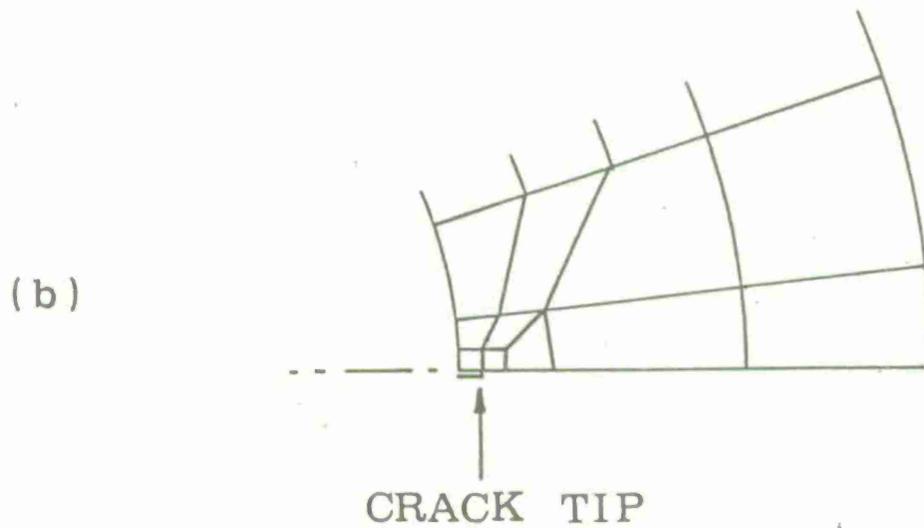Figure 1(a). A typical finite element idealization.

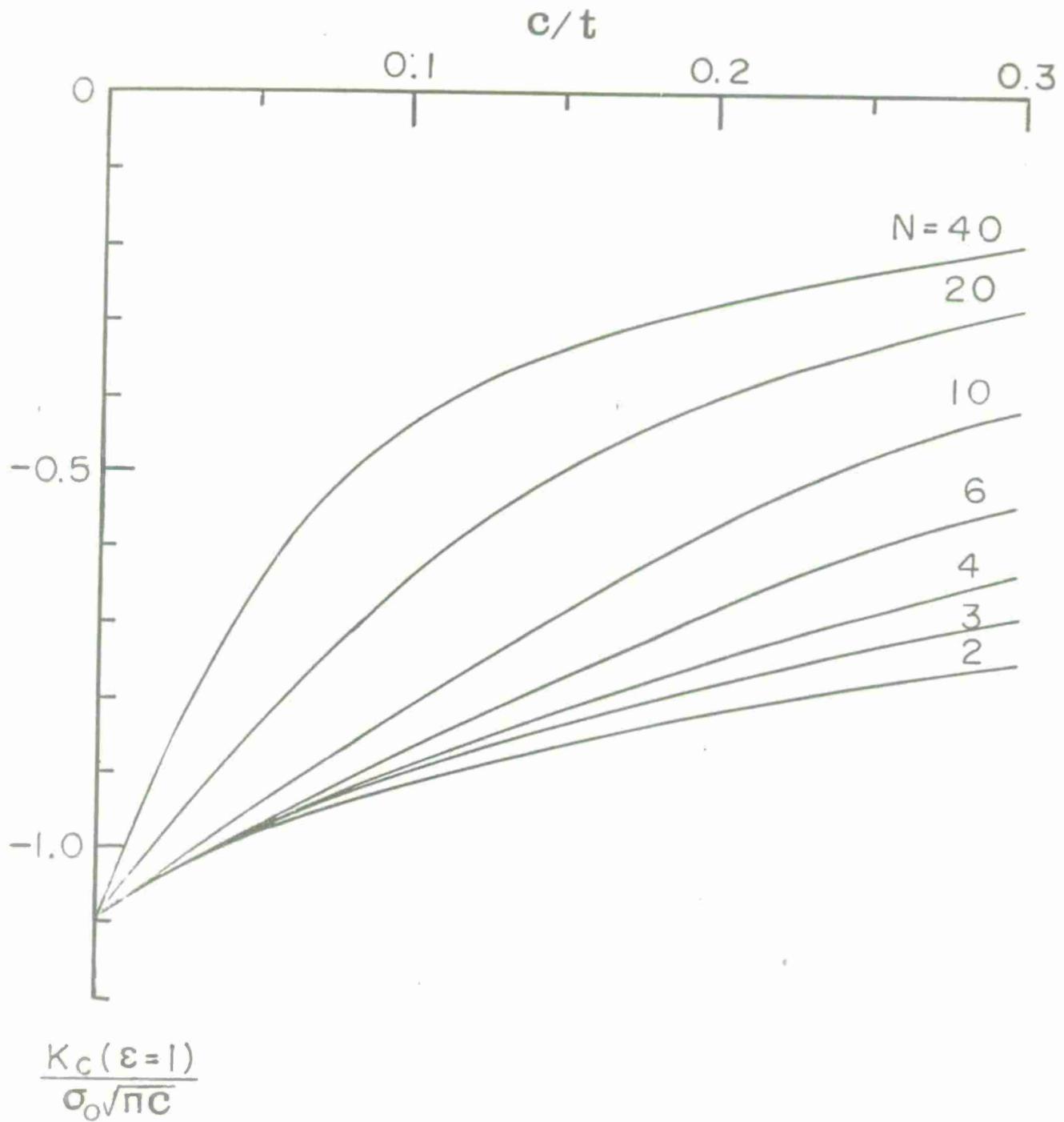CRACK TIP

Figure 1(b). Idealization for very shallow cracks.

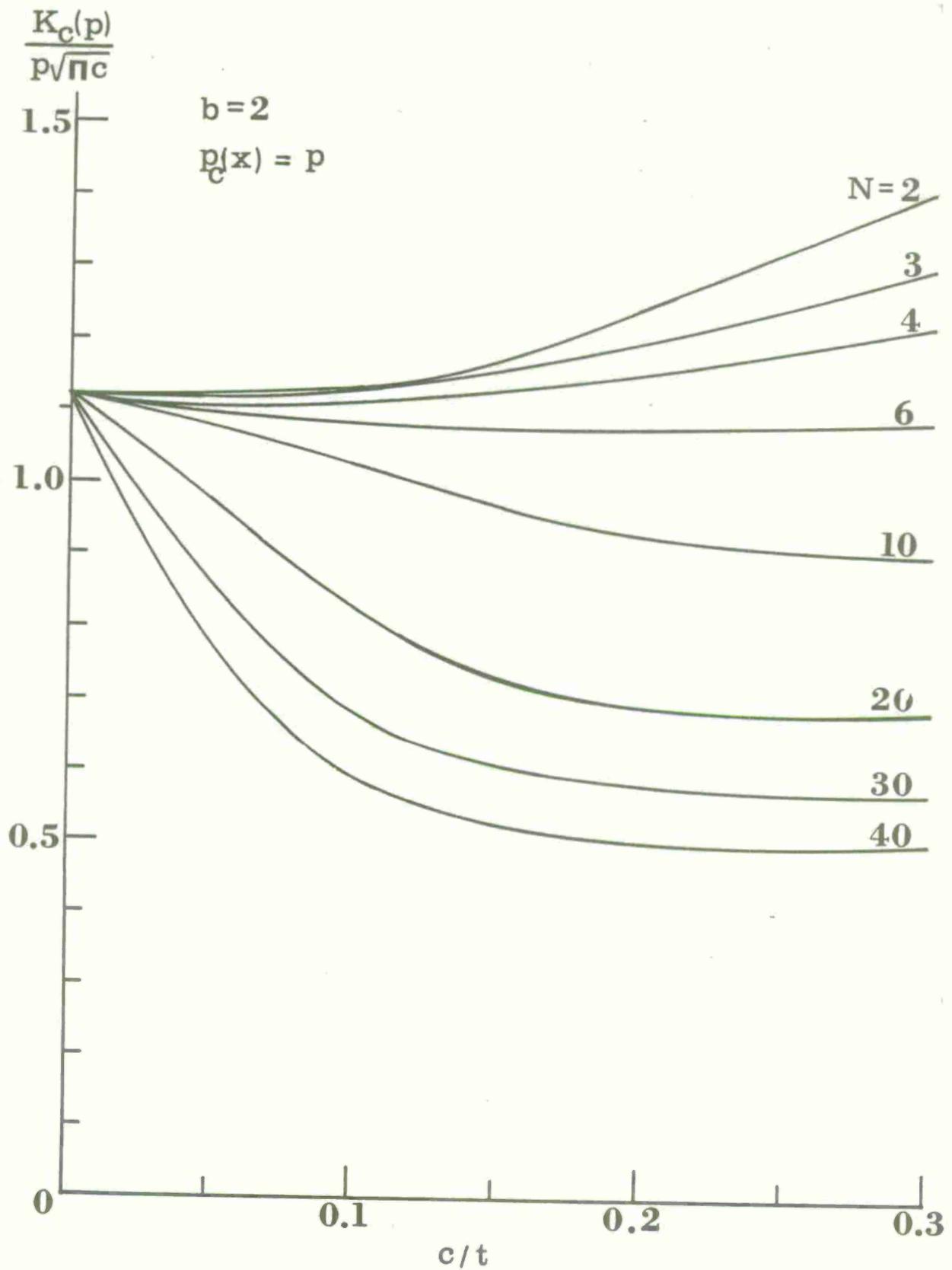Figure 2. Stress intensity factor as a function of c/t for N ID cracks in a fully autofrettaged cylinder of b/a = 2.

Figure 3. $K_c/p\sqrt{\pi c}$ as a function of c/t for N internal radial cracks with constant crack face loading.
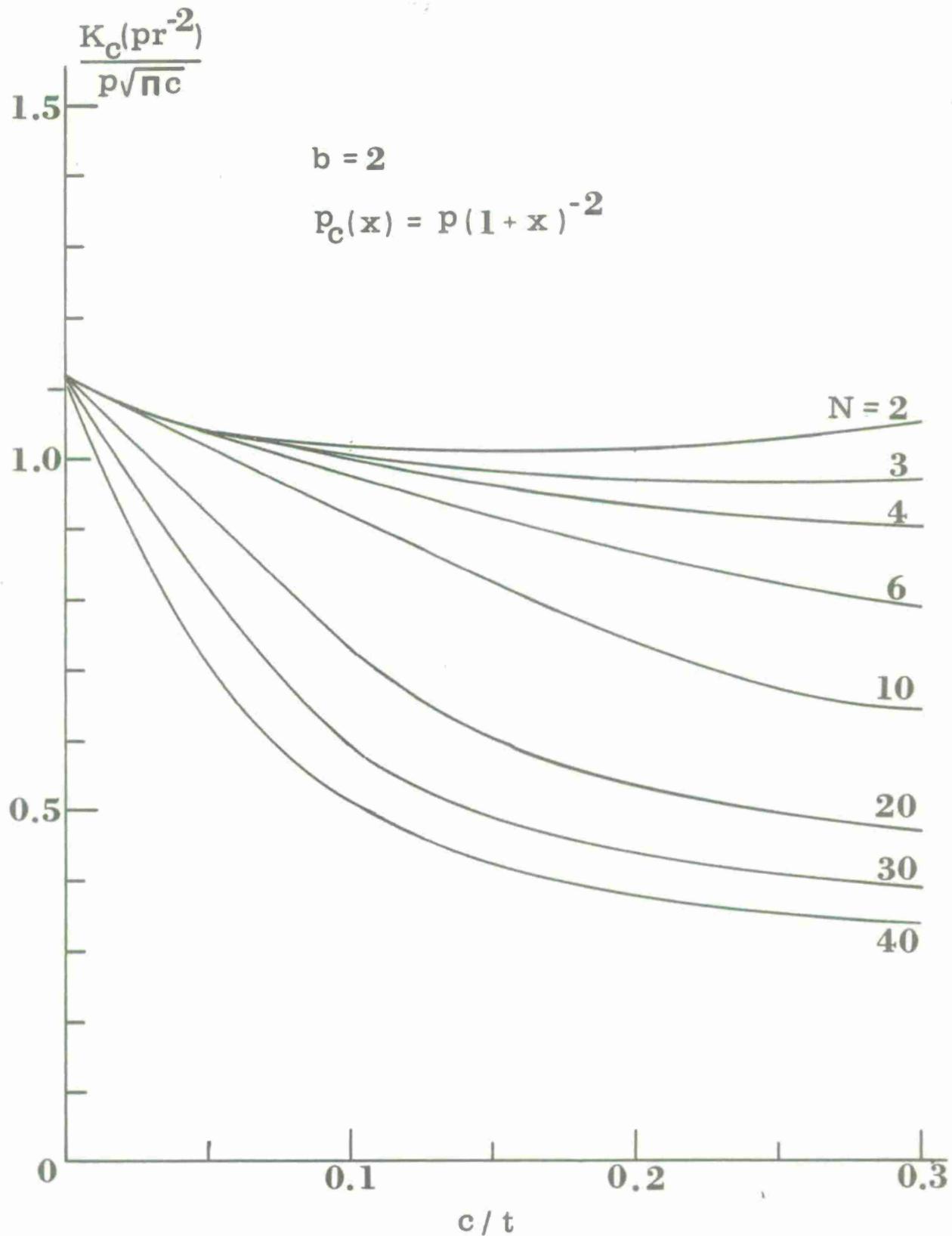
18

Figure 4. $K_c/p\sqrt{\pi c}$ vs. c/t for N internal radial cracks with crack face loading $p_c(x) = p(1+x)^2$.
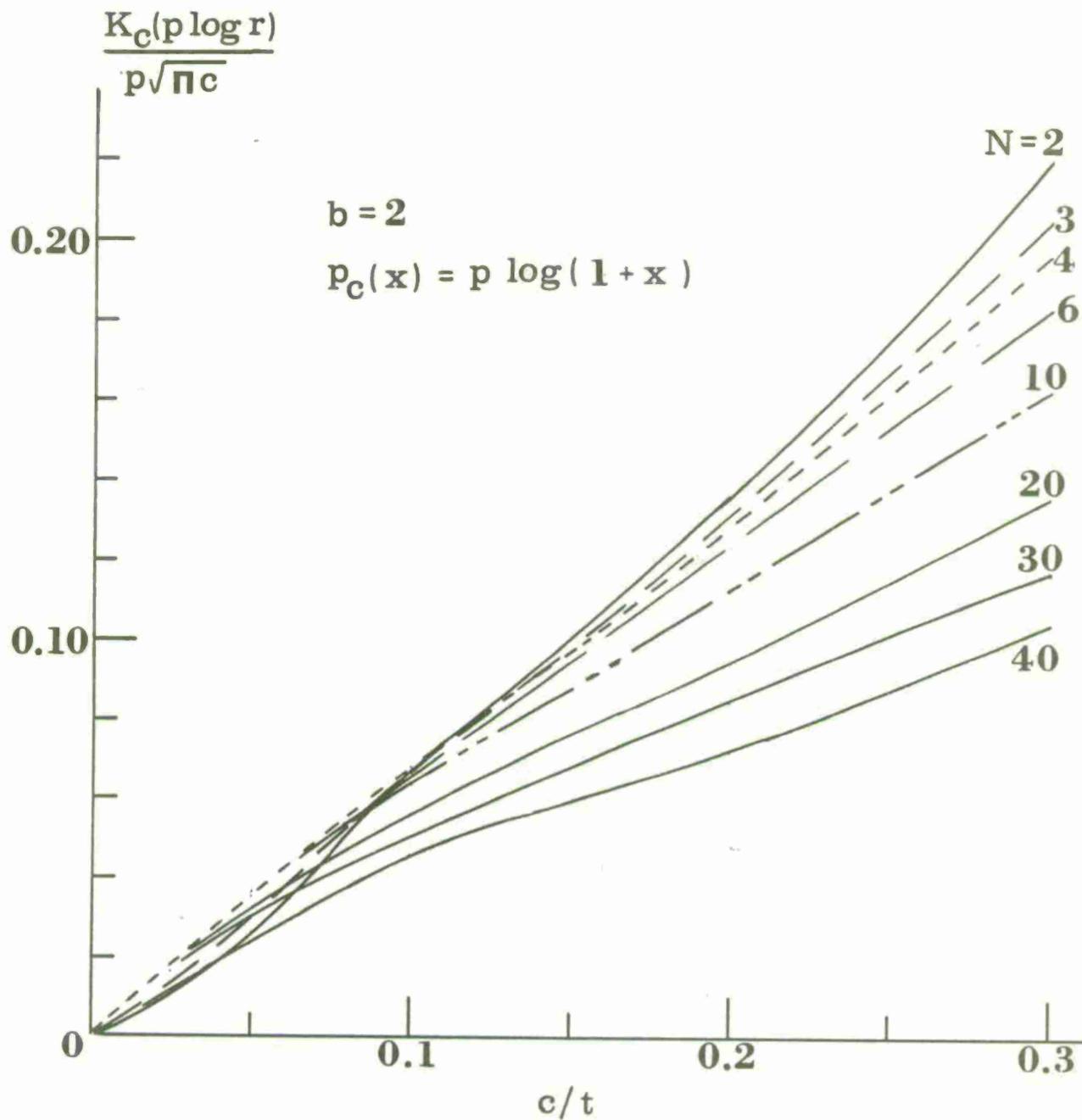
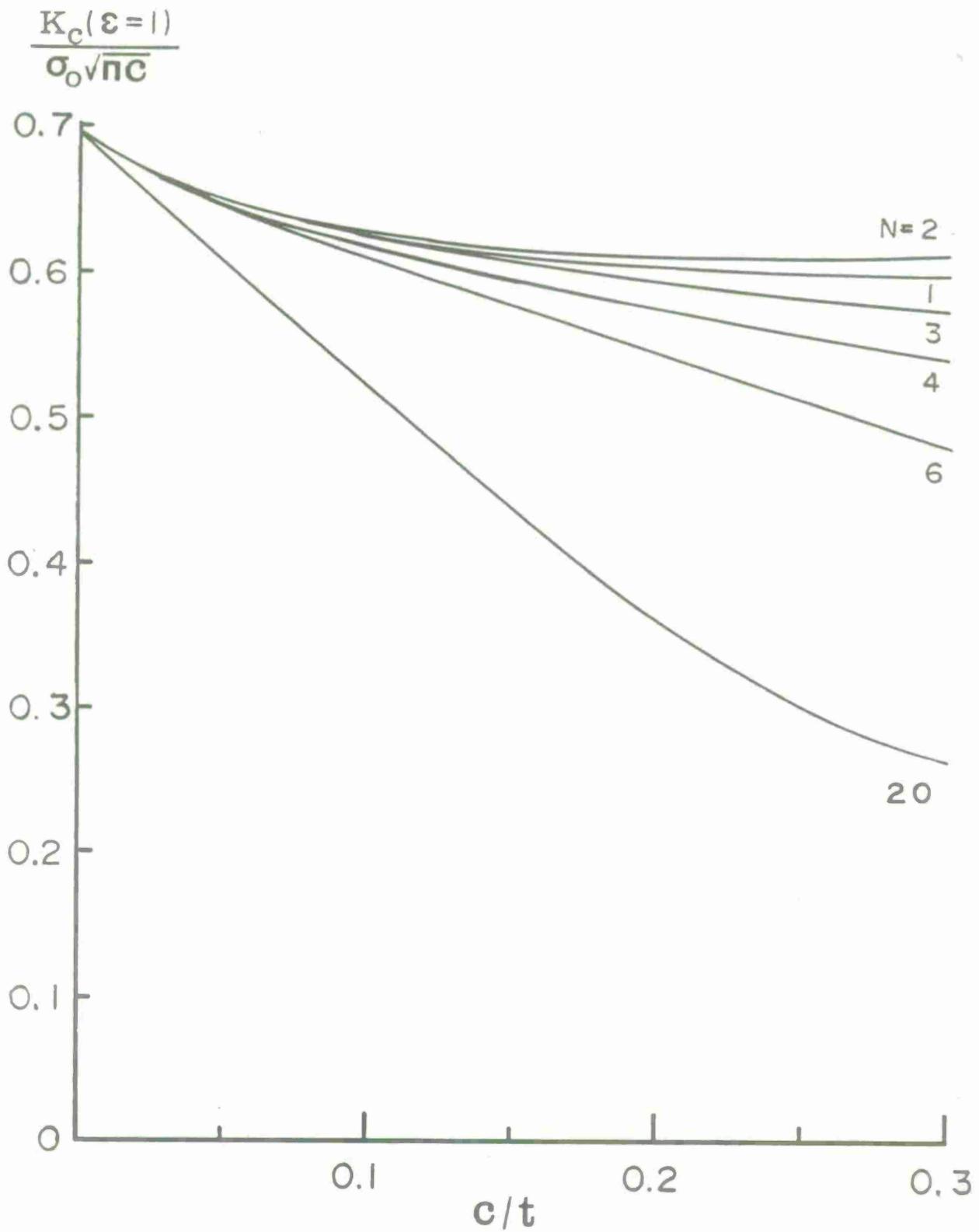Figure 5. $K_c/p\sqrt{\pi c}$ vs. c/t for N internal radial cracks with crack face loading $p_c(x) = p \log(1+x)$.

Figure 6. $K/\sigma_0\sqrt{\pi c}$ as a function of c/t for N radial cracks at outer surface of a fully autofrettaged cylinder of $b/a = 2$.
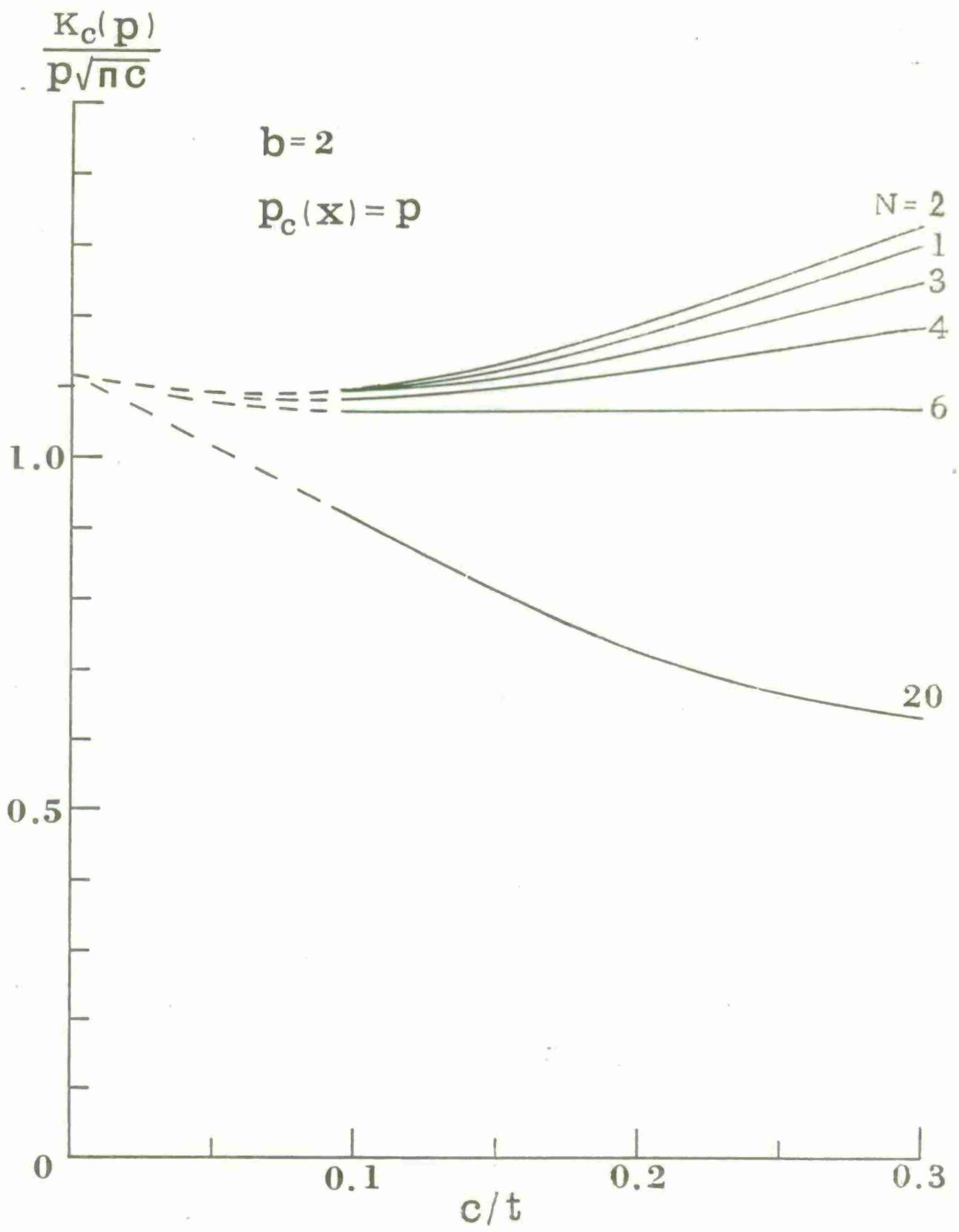
Figure 7. $K_c(p)/p\sqrt{\pi c}$ as a function of c/t for N external radial cracks with constant crack face loading.
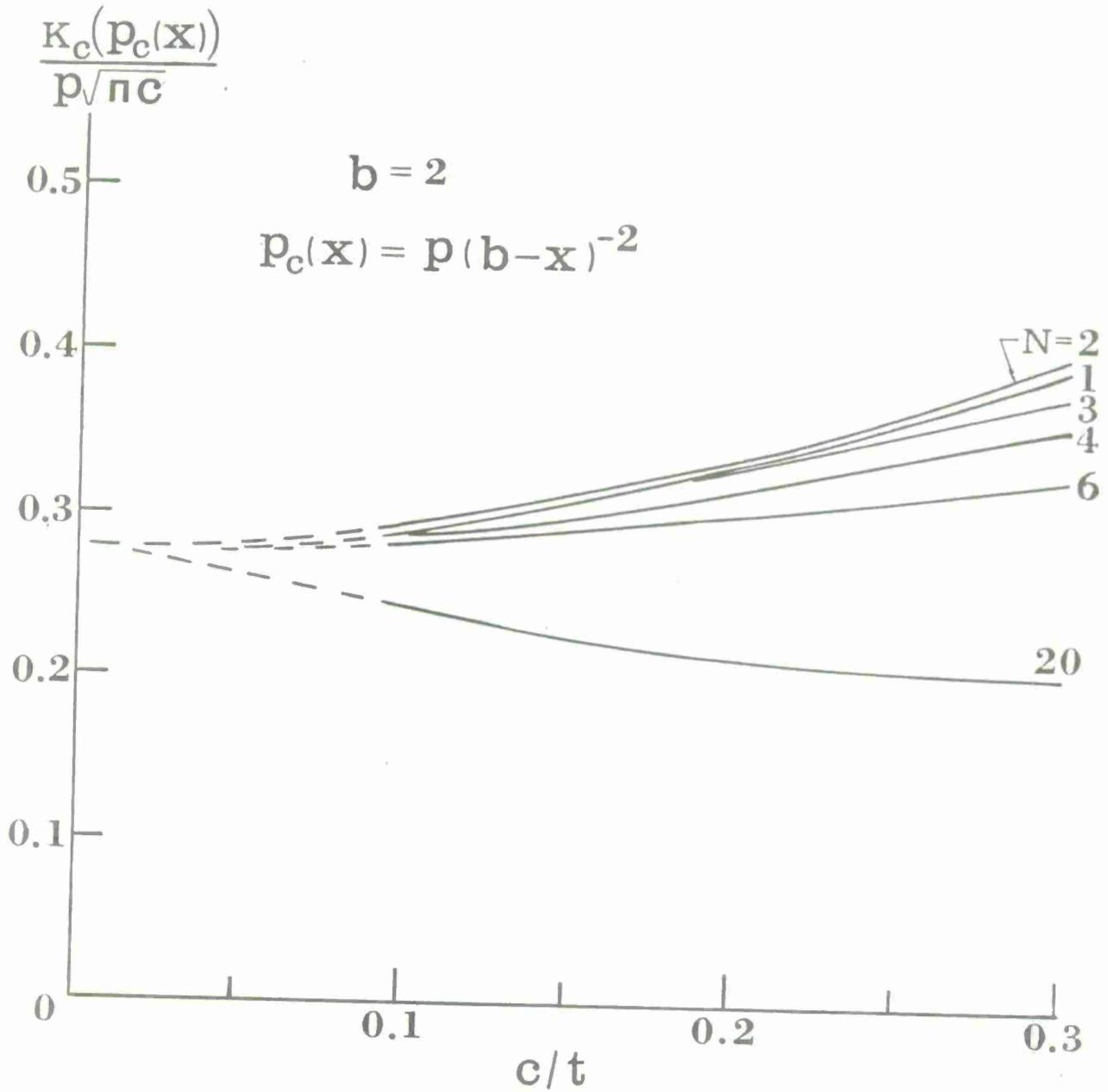
Figure 8. $K_c/p\sqrt{\pi c}$ vs. c/t for N external radial cracks with crack face loading $p_c(x) = p(b-x)^{-2}$.
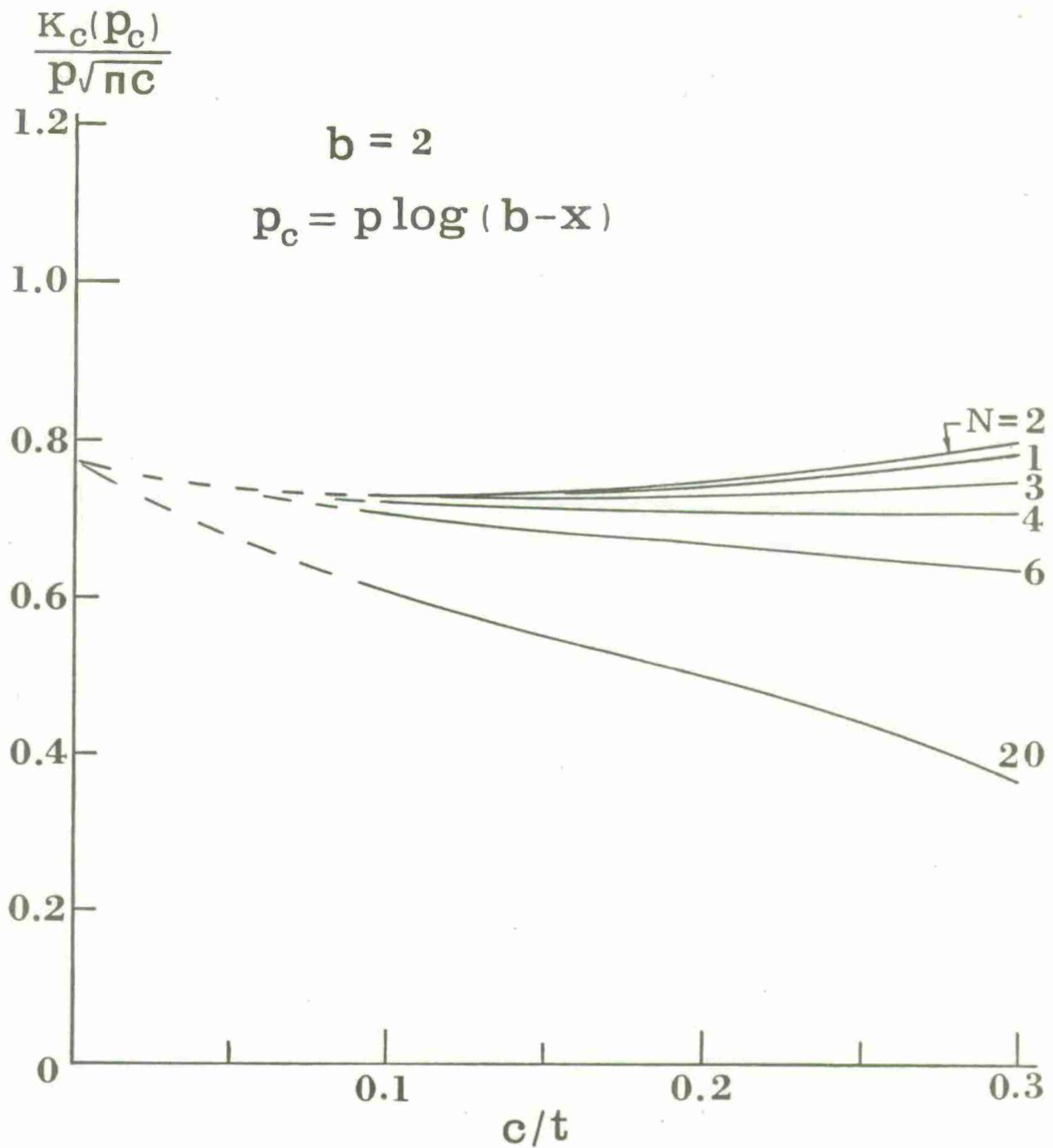
23

Figure 9. $K_c/p\sqrt{\pi c}$ vs. c/t for N external radial cracks with crack face loading $p_c(x) = p \log(b-x)$.

Figure 10. $K/\sigma_0\sqrt{\pi c}$ for N radial cracks at inner surface of a cylinder of b/a = 2 subjected to combined internal pressure $p_i = \sigma_0/f$ and residual stresses corresponding to given degrees of autofrettage, ε.
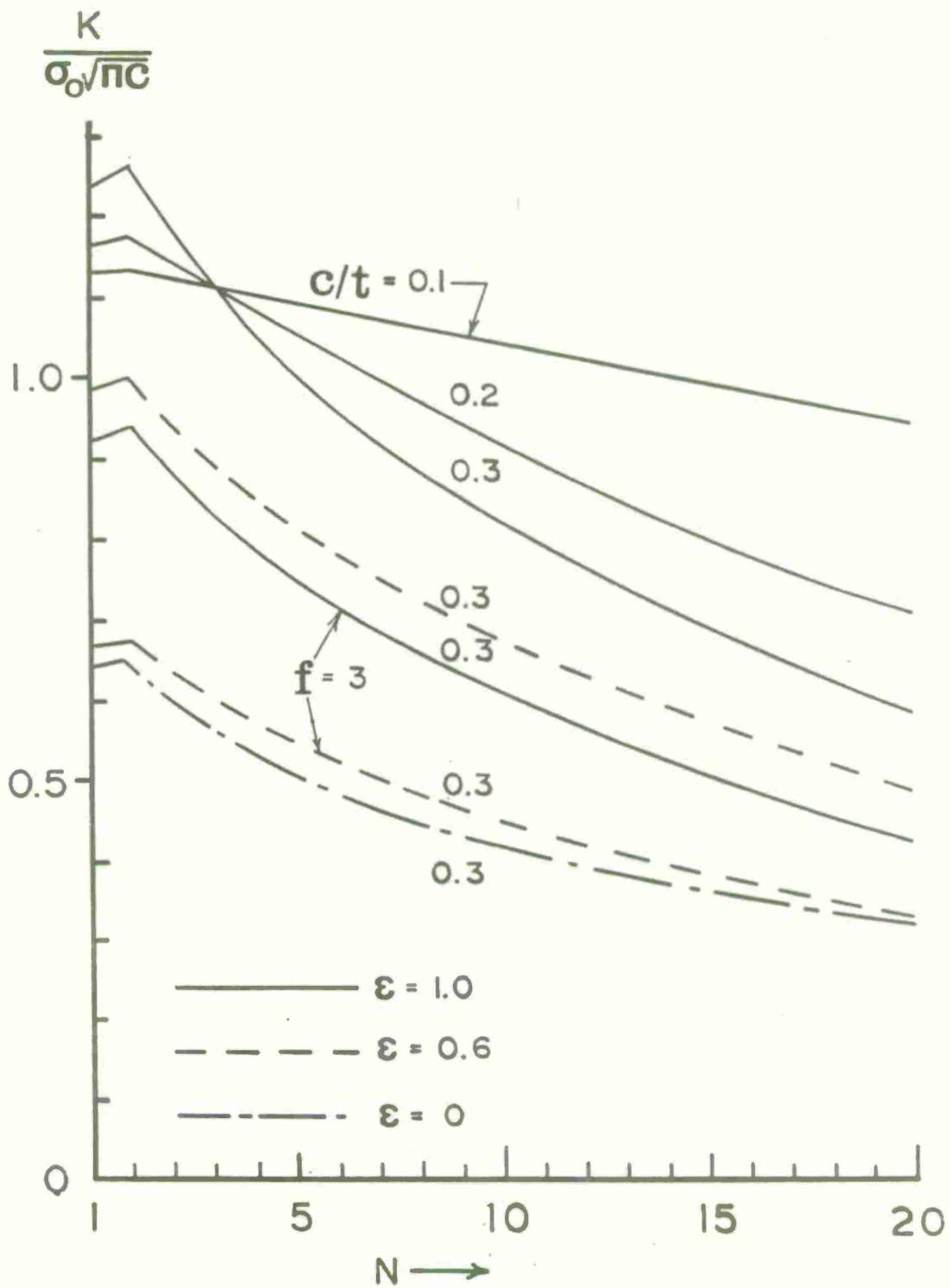
Figure 11. $K/\sigma_o\sqrt{\pi c}$ for N radial cracks at outer surface of a cylinder of $b/a = 2$ subjected to combined internal pressure $p_i = \sigma_o/f$, where $f = 1.5$ except otherwise indicated, and residual stresses corresponding to given degrees of autofrettage ε.

TECHNICAL REPORT INTERNAL DISTRIBUTION LIST

	NO. OF COPIES
CHIEF, DEVELOPMENT ENGINEERING BRANCH	
ATTN: DRDAR-LCB-D	1
-DP	1
-DR	1
-DS (SYSTEMS)	1
-DS (ICAS GROUP)	1
-DC	1
CHIEF, ENGINEERING SUPPORT BRANCH	
ATTN: DRDAR-LCB-S	1
-SE	1
CHIEF, RESEARCH BRANCH	
ATTN: DRDAR-LCB-R	2
-R (ELLEN FOGARTY)	1
-RA	1
-RM	1
-RP	1
-RT	1
TECHNICAL LIBRARY	5
ATTN: DRDAR-LCB-TL	
TECHNICAL PUBLICATIONS & EDITING UNIT	2
ATTN: DRDAR-LCB-TL	
DIRECTOR, OPERATIONS DIRECTORATE	1
DIRECTOR, PROCUREMENT DIRECTORATE	1
DIRECTOR, PRODUCT ASSURANCE DIRECTORATE	1

NOTE: PLEASE NOTIFY DIRECTOR, BENET WEAPONS LABORATORY, ATTN: DRDAR-LCB-TL,
    OF ANY REQUIRED CHANGES.

TECHNICAL REPORT EXTERNAL DISTRIBUTION LIST

	NO. OF COPIES		NO. OF COPIES
ASST SEC OF THE ARMY RESEARCH & DEVELOPMENT ATTN: DEP FOR SCI & TECH THE PENTAGON WASHINGTON, D.C. 20315	1	COMMANDER ROCK ISLAND ARSENAL ATTN: SARRI-ENM (MAT SCI DIV) ROCK ISLAND, IL 61299	1
COMMANDER DEFENSE TECHNICAL INFO CENTER ATTN: DTIC-DDA CAMERON STATION ALEXANDRIA, VA 22314	12	DIRECTOR US ARMY INDUSTRIAL BASE ENG ACT ATTN: DRXIB-M ROCK ISLAND, IL 61299	1
COMMANDER US ARMY MAT DEV & READ COMD ATTN: DRCDE-SG 5001 EISENHOWER AVE ALEXANDRIA, VA 22333	1	COMMANDER US ARMY TANK-AUTMV R&D COMD ATTN: TECH LIB - DRSTA-TSL WARREN, MI 48090	1
COMMANDER US ARMY ARRADCOM ATTN: DRDAR-LC	1	COMMANDER US ARMY TANK-AUTMV COMD ATTN: DRSTA-RC WARREN, MI 48090	1
DRDAR-LCA (PLASTICS TECH EVAL CEN) DRDAR-LCE DRDAR-LCM (BLDG 321) DRDAR-LCS DRDAR-LCU DRDAR-LCW DRDAR-TSS (STINFO) DOVER, NJ 07801	1 1 1 1 1 1 2	COMMANDER US MILITARY ACADEMY ATTN: CHM, MECH ENGR DEPT WEST POINT, NY 10996 US ARMY MISSILE COMD REDSTONE SCIENTIFIC INFO CEN ATTN: DOCUMENTS SECT, BLDG 4484 REDSTONE ARSENAL, AL 35898	1 2
DIRECTOR US ARMY BALLISTIC RESEARCH LABORATORY ATTN: DRDAR-TSB-S (STINFO) ABERDEEN PROVING GROUND, MD 21005	1	COMMANDER US ARMY FGN SCIENCE & TECH CEN ATTN: DRXST-SD 220 7TH STREET, N.E. CHARLOTTESVILLE, VA 22901	1
COMMANDER US ARMY ARRCOM ATTN: DRSAR-LEP-L ROCK ISLAND ARSENAL ROCK ISLAND, IL 61299	1	COMMANDER US ARMY MATERIALS & MECHANICS RESEARCH CENTER ATTN: TECH LIB - DRXMR-PL WATERTOWN, MA 02172	2

NOTE: PLEASE NOTIFY COMMANDER, ARRADCOM, ATTN: BENET WEAPONS LABORATORY,
DRDAR-LCB-TL, WATERVLIET ARSENAL, WATERVLIET, NY 12189, OF ANY
REQUIRED CHANGES.

	NO. OF COPIES		NO. OF COPIES
COMMANDER US ARMY RESEARCH OFFICE ATTN: CHIEF, IPO P.O. BOX 12211 RESEARCH TRIANGLE PARK, NC 27709	1	DIRECTOR US NAVAL RESEARCH LAB ATTN: DIR, MECH DIV CODE 26-27 (DOC LIB) WASHINGTON, D.C. 20375	1 1
COMMANDER US ARMY HARRY DIAMOND LAB ATTN: TECH LIB 2800 POWDER MILL ROAD ADELPHIA, MD 20783	1	METALS & CERAMICS INFO CEN BATTELLE COLUMBUS LAB 505 KING AVE COLUMBUS, OH 43201	1
COMMANDER NAVAL SURFACE WEAPONS CEN ATTN: TECHNICAL LIBRARY CODE X212 DAHLGREN, VA 22448	1	MATERIEL SYSTEMS ANALYSIS ACTV ATTN: DRXSY-MP ABERDEEN PROVING GROUND MARYLAND 21005	1

NOTE: PLEASE NOTIFY COMMANDER, ARRADCOM, ATTN: BENET WEAPONS LABORATORY, DRDAR-LCB-TL, WATERVLIET ARSENAL, WATERVLIET, NY 12189, OF ANY REQUIRED CHANGES.

READER EVALUATION

Please take a few minutes to complete the questionnaire below and return to us at the following address: Commander, U.S. Army ARRADCOM, ATTN: Technical Publications, DRDAR-LCB-TL, Watervliet, New York 12189.

1. Benet Weapons Lab. Report Number _____

2. Please evaluate this publication (check off one or more as applicable).

	Yes	No
Information Relevant	_____	_____
Information Technically Satisfactory	_____	_____
Format Easy to Use	_____	_____
Overall, Useful to My Work	_____	_____
Other Comments	_____	

_____

_____

3. Has the report helped you in your own areas of interest? (i.e. preventing duplication of effort in the same or related fields, savings of time, or money). _____

_____

_____

4. How is the report being used? (Source of ideas for new or improved designs. Latest information on current state of the art, etc.). _____
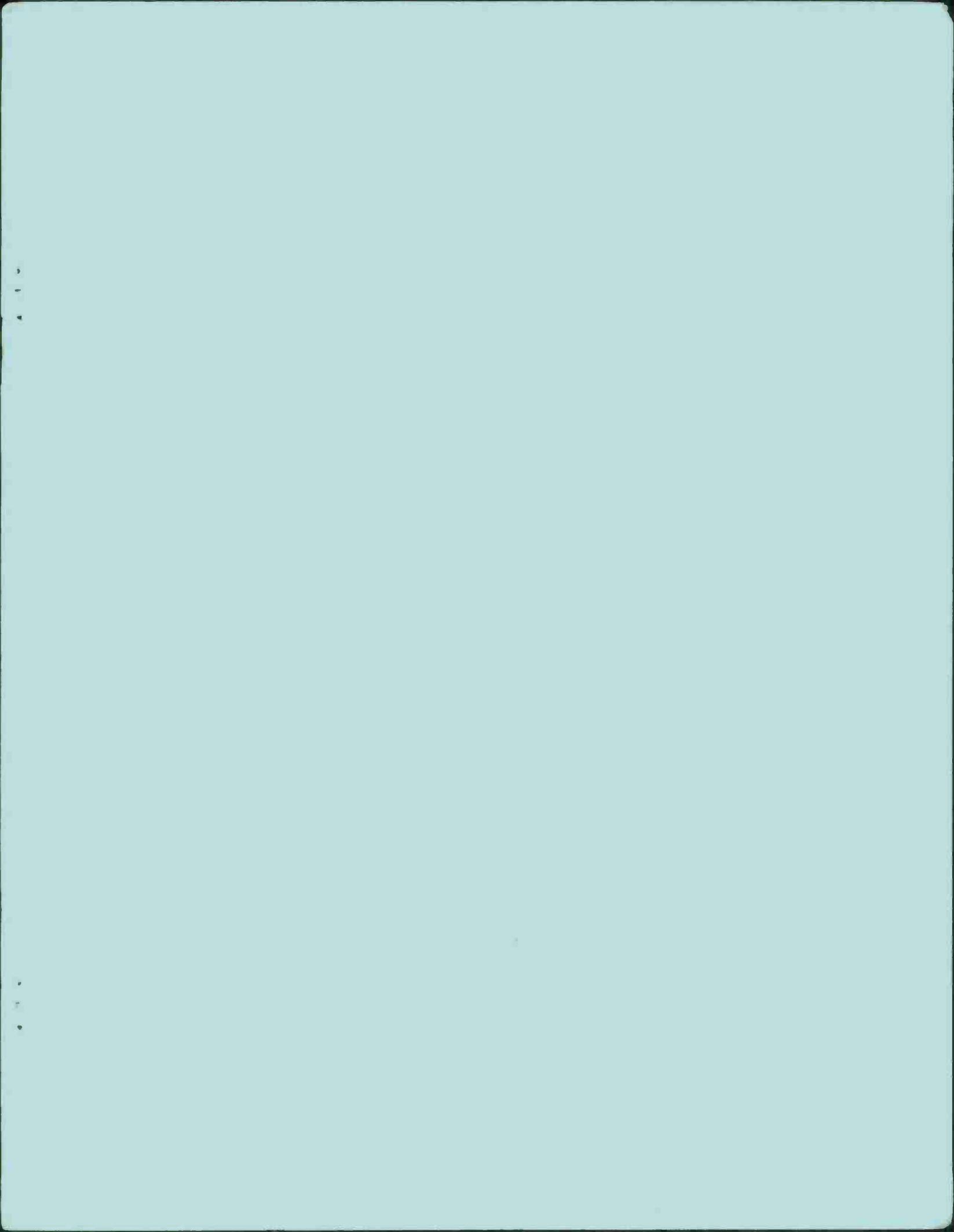
_____

_____

5. How do you think this type of report could be changed or revised to improve readability, usability? _____

_____

_____

6. Would you like to communicate directly with the author of the report regarding subject matter or topics not covered in the report? If so please fill in the following information.

   Name: _____

   Telephone Number: _____

   Organization Address: _____

   _____